HHS Public Access

Author manuscript

Environ Sci Nano. Author manuscript; available in PMC 2016 June 01.

Published in final edited form as:

Environ Sci Nano. 2015 June 1; 2(3): 262–272. doi:10.1039/C4EN00210E.

An integrated methodology for the assessment of environmental health implications during thermal decomposition of nano-enabled products

Georgios A. Sotiriou[1], **Dilpreet Singh**[1], **Fang Zhang**[1], **Wendel Wohlleben**[1,2], **Marie-Cecile G. Chalbot**[3], **Ilias G. Kavouras**[3], and **Philip Demokritou**[1,*]

[1]Center for Nanotechnology and Nanotoxicology, Department of Environmental Health, School of Public Health, Harvard University, 665 Huntington Ave., Boston, MA 02115, USA

[2]BASF SE, Material Physics, 67056 Ludwigshafen, Germany

[3]Department of Environmental and Occupational Health, College of Public Health, University of Arkansas for Medical Sciences, Little Rock, AR 72205, USA

Abstract

The proliferation of nano-enabled products (NEPs) renders human exposure to engineered nanomaterials (ENMs) inevitable. Over the last decade, the risk assessment paradigm for nanomaterials focused primarily on potential adverse effect of pristine, as-prepared ENMs. However, the physicochemical properties of ENMs may be drastically altered across their life-cycle (LC), especially when they are embedded in various NEP matrices. Of a particular interest is the end-of-life scenario by thermal decomposition. The main objective of the current study is to develop a standardized, versatile and reproducible methodology that allows for the systematic physicochemical and toxicological characterization of the NEP thermal decomposition. The developed methodology was tested for an industry-relevant NEP in order to verify its versatility for such LC investigations. Results are indicative of potential environmental health risks associated with waste from specific NEP families and prompt for the development of safer-by-design approaches and exposure control strategies.

INTRODUCTION

An increasing number of nano-enabled products (NEPs) are finding their way into the traditional aerospace, automotive, building construction, and food packaging industries, among others.[1] Many industrial sectors are adopting a variety of engineered nanomaterials (ENMs) for improved strength, weight, texture, biocidal and optical properties tailored to specific applications.[2–3] Examples of such NEPs include paint coatings, with a variety of submicron/nanoscale pigment (metal and oxide) powders;[4] toner formulations;[5–7] polymer- and carbon-matrix nanocomposites;[8] sintered compacts made of metal and oxide nanoparticles;[9] super hard coatings.[10]

Corresponding author: pdemokri@hsph.harvard.edu.

Supporting Information is available with detailed experimental section and the results of the physicochemical characterization of the released aerosol.

Recent evidence and historic data demonstrate the potential for ENMs to elicit adverse biological and environmental effects.[11–15] Engineered nanoparticles and nanofibers may translocate across biological barriers reaching pulmonary connective tissues, lymphatics, or even the circulating blood and thus gain access to other critical organs.[16–18] Whereas the chemical composition plays an important role for the inflammatory potential,[19] nanoparticles may enter cells and be more biologically active than their larger counterparts due to their small size and large surface-to-volume ratio.[20–24]

Nano-environmental health and safety (nano-EHS) research has expanded over the last decade; yet, underlying mechanisms for nano-EHS interactions are starting to emerge.[25] Major knowledge gaps still exist.[26] More specifically, the current “modus operandi” in the nano-risk assessment paradigm focuses only on the pristine (raw) ENMs. This is not appropriate to address possible adverse health effects associated with NEPs across their life-cycle (LC). This important knowledge gap has been recently emphasized in both the National Research Council report, as well as in the National Nanotechnology Initiative’s strategy on nano-EHS.[27–28] During potential “cradle to grave” LC exposure scenarios for NEPs,[29] a mixture of possible pollutants will be generated which may include particulate matter (PM) of different sizes with or without a nanoscale fraction, as well as other gaseous co-pollutants (e.g. volatile organic compounds (VOCs) and semi-volatile organic compounds (sVOCs)). These nano-EHS uncertainties surrounding LC implications of NEPs, if unaddressed, will impede public health assessors from addressing nano-related risk issues. This will have implications at societal and economic levels as well as on the sustainable development of the nanotechnology industry. Thus, new methodological approaches are urgently needed to address LC implications of NEPs.

Only a handful of ENM exposure/release studies across LC continuum exist and focus primarily on carbon nanotubes (CNTs) embedded in polymer systems. More importantly, there are no standardized methodologies in terms of performing this type of studies, neither there are exposure generation systems suitable for both physicochemical and toxicological characterization of NEPs across their LC. Most of the published studies characterize the properties of released PM under a limited number of release scenarios such as sanding, drilling, sawing, etc.[30–37]

One important and understudied end-of-life exposure scenario is the thermal decomposition (TD) of NEPs.[38] Recent studies on ENMs flows through society indicate that an important fraction of products containing ENMs will be disposed via thermal decomposition/ incineration,[39] particularly in Europe and North America.[40] It is estimated that up to 8,600 metric tons of ENMs per year are disposed in this manner worldwide and the volume is expected to grow exponentially in the years ahead. Although released fly ash and residual ashes are typically disposed in landfills, there are many countries without regulations, or where these regulations are not well enforced. Another concern is the incomplete TD, due to poor operating practices, or incidental fires of NEPs in various settings such as buildings that may produce toxic air and soil emissions. The mobility and fate of TD byproducts containing ENMs in the environment is poorly understood and may pose potential threats to environmental media and human health.[41]

There is limited literature on the TD of nanomaterials with only three published studies[38,41–42] but evidence continues to grow. Walser et al.[41] investigated the fate of raw CeO_2 nanoparticles upon their disposal in an incineration plant. They found that CeO_2 particles do not escape in the atmosphere during incineration, but might bind to waste residues and end-up in landfills. Regarding polymer nanocomposites, Bouillard et al.[38] studied the potential release of CNTs from CNT-polymer composites upon their controlled combustion. The particle size distribution of the resulting aerosol is sub-micron, with a large fraction in the nano-regime (<100 nm). At specific combustion conditions, the released aerosol was primarily identified as soot nanoparticles (10–30 nm) including the release of some CNTs. Vejerano et al.[42] investigated the incineration of nanomaterials when added in surrogate wastes and found that very little amount of the ENM escapes in the released aerosol PM and most of them remain in the residual ash after incineration.

However, our understanding of the important parameters affecting the possible release of nanofillers used in the synthesis of NEPs, the role of matrices and thermal decomposition conditions on the properties of byproducts and their biological properties has not been investigated so far. Generating this necessary new knowledge requires a rigorous and multidisciplinary approach combining LC concepts with material and aerosol science, exposure, environmental and biological assessment. In order to fill this large knowledge gap, we need to: 1) Identify priority NEPs currently on the market with the potential to end up in incineration facilities; 2) Develop “best practice” methods suitable for the generation, physicochemical and toxicological characterization of realistic exposures associated with TD of NEPs; 3) Demonstrate the reproducibility of these methods and build our knowledge of factors influencing nano-release for representative classes of materials; and 4) Utilize the developed methods and knowledge to generate “safer-by-design”[43–44] NEPs and exposure control strategies.

Knowledge gaps and research strategy

There are several questions/hypotheses that need to be addressed regarding the thermal decomposition of NEPs and possible environmental, health and safety implications of such byproducts:

1. What are the physicochemical and morphological properties of the released aerosol during TD of industry relevant NEPs?
2. Are any nanofillers released from NEP and under what TD process conditions ?
3. How does the presence of s/VOCs from combustion of matrices used in the synthesis of NEPs influence the released aerosol chemical composition and toxicity?
4. What is the physicochemical and morphological characterization of the residual ash ? Are there nanofillers remained in the residual ash after TD and at what concentration and condition?
5. How does the properties of nanofillers and matrices used in the synthesis of NEPs influence the physicochemical, morphological and toxicological properties of the byproducts

6. What is the toxicological profile of the released aerosol and the residual ash? Is there a nanofiller-specific effect?

7. What is the fate and transport of the residual ash in the environment?

In order to provide valuable data on the above questions for industry relevant families of NEPs, proper methodology and integrated systems need to be developed that allow for systematic and reproducible investigation. The main target of this study is to develop an integrated generation platform that allows for the systematic and reproducible investigation of the TD of NEPs in order to obtain a fundamental understanding on this process. We present here the main features of the developed system and perform a case-study for a commonly used NEP, cross-linked polyurethane filled with multiwall carbon nanotubes (PU-CNT, Supporting Information, Figure S1),[37] in order to prove its versatility in LC assessment studies. Such an NEP is currently in use in many industrial products that require both toughness, elasticity and conductivity.

MATERIALS & METHODS

Detailed description of the components of the developed system, the NEP preparation and characterization, as well as the physicochemical characterization of the released aerosol and residual ash are available in the Supporting Information.

Integrated exposure generation system (INEXS)

Figure 1 shows the main components of INEXS system. The NEP is placed in a quartz crucible and placed in a tube furnace (furnace #1). The inlet gas of this furnace could be either HEPA filtered ambient air, or of a controlled atmosphere (e.g. O_2/N_2 ratio) in order to simulate both incomplete and complete combustion conditions. The final decomposition temperature $T_{d,final}$ and heating rate in furnace #1 can be precisely controlled. The $T_{d,final}$ can be selected to any temperature up to 1200 °C, even though in this study we selected two values, 500 and 800 °C. As the temperature in furnace #1 increases and the NEP decomposes, both gaseous pollutants and aerosol PM is released. The gas composition is monitored in real time at the exit of furnace #1 (e.g. CO, O_2, CO_2). By monitoring the O_2 content, it is ensured that the O_2 content remains at the desired levels throughout the whole experiment to ensure complete or incomplete combustion scenarios.

Following the exit of furnace #1, the released aerosol may pass through three different routes to simulate various operational scenarios and conditions. Route I induces no further treatment to the released aerosol and best reflects TD scenarios of accidental fires and/or incineration of NEPs. In route II, the released aerosol passes through a thermal denuder, which is used to remove s/VOCs from the released aerosol. This route enables the investigation of the s/VOCs effect on the released aerosol physicochemical characteristics and subsequently on their biological responses and will help in assessing questions on the role of matrix on EHS matters. The PM aerosol is heated up to 300 °C in the thermal denuder and s/VOCs are vaporized from particles and then adsorbed on activated charcoal. It is worth mentioning that s/VOCs are expected to exist as a byproduct of TD of organic compounds currently in use in the synthesis of many families of NEPs (i.e., thermoplastics, coatings) similarly to generated aerosol from diesel exhaust engines.[45]

Route III enables an additional processing step of the released aerosol. The released aerosol passes through a thermal conditioner which consists of a tube furnace that can further heat the aerosol up to 1100 °C. This additional processing step is designed as such in order to best reflect the afterburner conditions at a commercial incineration facility (at least 5 s residence time at 800 °C).[46]

Independent of the chosen route/scenario (I, II, III), the released aerosol is then guided to a series of *in situ*, real-time particle characterization instrumentation which enables measurement of particles from 2 nm to 20 μm. More specifically, the released aerosol particle concentration and size distribution are monitored in real time using a scanning mobility particle sizer and an aerodynamic particle sizer for the nano- and micron-sized regime, respectively. Before each instrument, the released aerosol is further diluted using a rotating disk diluter prior to the SMPS and an aerosol diluter prior to the APS (100:1 dilution), in order to ensure that the aerosol concentration is in measurable levels. The presence of any total volatile organic compounds (tVOCs) is also monitored in real time.

Apart from the *in situ*, real-time particle characterization, the released aerosol can also be size fractionated and collected using the Harvard compact cascade impactor (CCI).[47] This impactor fractionates and collects the released aerosol in desired size ranges (e.g. $PM_{0.1}$, $PM_{0.1–2.5}$, $PM_{>2.5}$). This is important because different size fractions may exhibit different chemical composition and deposition dynamics in the lung when inhaled. TEM grids may be placed on each stage of the CCI sampler further providing evidence of the size and morphology of the released aerosol. Furthermore, another important feature of the CCI, is its ability to collect large amounts of size fractionated PM (mg range) on specific polyurethane foam (PUF) substrates ($PM_{>0.1}$) and Teflon/quartz filters ($PM_{0.1}$) which are needed for the toxicological characterization of the released aerosol.[47] The size fractionated sampled PM will then be extracted using previously developed protocols[48–49] and used both for the off-line physicochemical and toxicological characterization of the released aerosol.

It is noteworthy that the released aerosol may be also directed in animal chambers for *in vivo* inhalation toxicological studies, similarly to studies performed previously with pristine aerosol engineered nanomaterials.[11,13] Such *in vitro* cellular and *in vivo* inhalation toxicological studies are crucial and as mentioned above, will help in particular in identifying whether there is a specific nanofiller toxicological effect in addition to potential effects from gaseous emissions which is the case for pure polymers.[50]

RESULTS AND DISCUSSION

Physicochemical characteristics of released aerosol and residual ash

Released aerosol concentration and size as a function of thermal decomposition temperature—Figure 2 shows the time evolution of TD temperature ($T_{d,final}$, furnace #1) of the NEP (left axis, red line). Two final temperatures were investigated, $T_{d,final}$ = 500 (a) and $T_{d,final}$ = 800 °C (b). The particle number concentration as a function of time as measured by the SMPS (route I, right axis, black line) was also measured (dilution factor = 100). The error bars correspond to standard deviation from three individual measurements, further demonstrating the high reproducibility of the system. The

particle generation during thermal evolution starts occurring around 300 °C, independent of the final TD temperature ($T_{d,final}$). The maximum particle release occurs at ~400 °C for both $T_{d,final}$ conditions tested here (~10^6 #/cm^3). Beyond the 400 °C temperature the aerosol particle concentration decreases with time, as the combustion is close to completion. These results are in agreement with the gas composition monitoring the CO concentration during TD (Supporting Information, Figure S2).

Figure 3 shows the released aerosol particle size distribution (mobility diameter) for both $T_{d,final}$ = 500 (a) and 800 °C (b) at three different time points during the thermal decomposition process, along with their corresponding statistics. For both $T_{d,final}$ conditions the particle size distribution shifts from small sizes (solid lines in Figure 3a,b) to large sizes (dotted lines in Figure 3a,b) as time increases (and particle concentration, Figure 2a,b) reaching a maximum at ~400 °C (see also Supporting Information, Figure S3). This size increase is expected due to the higher particle coagulation at higher particle concentration levels. The average size of the released aerosol ranges from ~30 to ~100 nm, in agreement with the sizes observed in the literature.[38]

In addition to the released aerosol characterization in the nano-regime, the particle concentration and size was also monitored in the micro-regime. The particle number concentration in this regime (0.5 – 20 μm) is rather low, but not negligible (Supporting Information, Figure S4). This indicates that the released aerosol is rather polydisperse including particles with aerodynamic diameters >2.5 μm. The mass size distribution of the released aerosol was also measured using the CCI (Supporting Information, Figure S5).

Nanofiller release in the aerosol?—For the detection of any nanofillers in the released aerosol, a number of *ex situ* characterization techniques were employed. First, the size fractionated released aerosol that is collected on the PUF and/or filters is extracted in pure EtOH and then deposited on a Si substrate for SEM imaging. Figure 4 shows such representative images of the released aerosol after extraction for $PM_{0.1}$ (a,c) and $PM_{0.1–2.5}$ (b,d) for $T_{d,final}$ = 500 (a,b) and 800 °C (c,d). The particles have agglomerated in suspension forming large structures. The different nano-features are identified in both size fractions. There are no visible CNTs in these SEM images. The extraction and re-suspension of the released aerosol might not reflect best its size and morphology as potential transformation might occur during this procedure. It allows, however, for the investigation of a high fraction of the sample for the detection of potential released of CNTs. It should be noted that a large number of images (>50) have been obtained, and no CNTs were detected for this CNTs loading (0.09 wt%). However, this observation cannot be extrapolated for NEPS with higher CNT loadings.

Even though electron microscopy offers valuable morphological evaluation on the released aerosol, the obtained results are semi-quantitative. One way to quantify the CNT concentration is to detect the presence of the metal nanoparticles that act as catalyst during the CNT synthesis. The CNTs used as nanofiller here had a high concentration of Aluminum (Al, 4.37 ± 0.45 wt%, as determined by ICP-MS). Therefore, by measuring the Al content of the released aerosol, the CNT concentration can be quantified (assuming that there is no alteration of the Al concentration during the TD of the NEP). The Al content in the released

$PM_{0.1}$ aerosol for both $T_{d,final}$ conditions was found negligible (data not shown), further validating the absence of any CNTs as indicated by EM imaging. It should be noted that the absolute determination whether there are any CNTs present in the released aerosol is challenging, and therefore we may only state here that there were no CNTs present in the released aerosol given the detection limits of the techniques we employed.

Nanofiller presence in the residual ash?—It is worth noting that there is detectable residual ash only for $T_{d,final}$ = 500 °C condition. For the higher $T_{d,final}$ of 800 °C a full decomposition/combustion occurs and no residual ash was observed, as both the matrix (polymer) as well as the nanofiller are carbonaceous materials that fully combust in O_2-rich conditions at such a high temperature level. Figure 5 shows SEM images (a,b) of the residual ash at $T_{d,final}$ = 500 °C. The residual ash has the morphology of thin flakes that can be easily handled and evaluated by SEM. There are numerous CNT protrusions from the surface of the ash visible in the SEM images. In addition, when ultramicrotome cross-sections of the surface of the residual ash are examined by TEM (Figure 5c), the density of CNTs appears to be the same as on cross-sections of the bulk of residual ash (Figure 5d), indicating rather homogeneous distributions of CNTs throughout the whole flake. The ICP-MS analysis of the residual ash, indicates that the residual ash Al-content is 18 times higher than that in the raw initial PU-CNT (before the TD). This indicates that as the matrix is thermally degraded at this TD conditions the CNTs remain intact and enrich the residual ash. It is worth noting that the persistence of CNTs at 500°C is expected for multi-wall CNTs with high structural purity.[51–52]

Closing the mass balance for the nanofiller—It is worth noting that reporting the mass of byproducts from the TD process in a percentage of the waste is of great importance for further LC assessment (LCA) studies regarding the end-of-life of NEPs. There is currently a knowledge gap on this which limits our understanding in terms of potential environmental health implications.[40] In the case of PU-CNT, the initial NEP mass in furnace #1 was 100 ± 5 mg. The total mass of the released aerosol across the whole size range at $T_{d,final}$ = 500 and 800 °C was found to be 5.1 and 6.9 mg, respectively (5.1 and 6.9 %). In addition, the mass of the residual ash at $T_{d,final}$ = 500 °C was found to be 6.1 ± 1.4 mg (6.1 ± 1.4 %). The residual ash and released aerosol yields indicate that the remaining NEP mass was combusted to CO_2 and CO.

Given the fact that there were no detectable CNTs in the released aerosol for both temperatures and assuming that all CNTs in the initial PU-CNT (before TD, CNT loading: 0.09 wt%) remained in the residual ash, this will result in a corresponding CNT concentration in the residual ash in the range of 1.20 – 1.91 wt% (0.09 mg of CNT in 6.1 ± 1.4 mg). Furthermore, it is worth noting that from the ICP-MS results of the residual ash, the Al-content which is a tracer metal associated with the CNTs, was found to be 18 times higher than that of the initial PU-CNT sample before thermal decomposition, an indication that the CNT concentration in the residual ash is also 18 times higher. This corresponds to a 1.62 wt% CNT concentration in the residual ash, a value in the 1.20 – 1.91 wt% range per the calculation above. This is supportive of the hypothesis that at these thermal decomposition conditions ($T_{d,final}$ = 500 °C), most of CNTs remained in tact in the residual

ash and only the organic component of the NEP (in this case the PU) is decomposed releasing aerosol PM. One should be cautious, however, of such indirect quantification of CNTs in thermally-treated samples using the Al content as a surrogate because Al and the CNTs might behave differently at elevated temperatures. At $T_{d,final}$ = 500 °C conditions though, the use of Al content as a surrogate of the presence of CNTs is more likely to be closer to the real conditions as neither the multi-wall CNTs nor the Al should evaporate at this temperature. Further analytical techniques could be carried out for the CNTs quantification as performed recently by monitoring the C(1s) electron band with X-ray photoelectron spectroscopy.[37] On the other hand, the CNTs concentration here is rather low, which makes its accurate quantification in the residual ash a technical challenge.

Chemical analysis of released aerosol and residual ash—In order to further characterize the chemical composition of the released aerosol and residual ash, a number of characterization techniques were employed to measure the elemental and organic carbon content and organic chemical content. It is expected that a large fraction of the released aerosol will consist of organic carbonaceous compounds.[53] Indeed, the OC content of the released aerosol ($PM_{0.1}$) from the TD of PU-CNT at $T_{d,final}$ = 500 and 800 °C was found to be 99.2 ± 0.1%, independent of the $T_{d,final}$ indicating its little influence on the OC content. In contrast, the OC content of the residual ash at $T_{d,final}$ = 500 °C is only 17.95 % (EC = 82.05 %) as expected due to the polymer degradation/combustion. Even though the CNTs would be identified as EC in that analysis, they are not the dominating component in the residual ash since the initial CNT loading in the NEP was minimal (0.09 wt%).

To further characterize the effect of the organic carbonaceous components in the chemical composition of the released particles, a thermal denuder (route II in Figure 1) is included in the INEXS platform (Figure 1). Figure 6a shows the particle number concentration of the released aerosol after further processed by the denuder as a function of the mobility diameter at $T_{d,final}$ = 800 °C. It is apparent that the thermal denuder resulted to a 96.5% decrease of particle number concentration. This particle concentration decrease observed in route II (thermal denuder) is associated with the s/VOCs removal from the released aerosol and further verifies the high OC values obtained for this sample. In addition, the particle size distribution is also shifted to lower sizes, compared to the particle concentration/distribution before the denuder (route I, Figures 2b, 3b). These particles are formed primarily by homogenous nucleation and are organic in nature as indicated in the EC/OC analysis and were removed by the thermal denuder. It is worth noting that the particle losses through the denuder as a function of size were also assessed in separate experiments and were found to be between 30 – 50% for the size range of the released aerosol (please see Supporting Information for detailed experiments and calculations regarding the denuder particle losses, Figures S6, S7). Therefore, the decreased particle number concentration after the denuder (route II) can not only be attributed to particle losses, but also to the efficient removal of those s/VOC based particles. This is also verified by monitoring the tVOC concentration (GrayWolf Sensing Solutions) before and after the thermal denuder as seen in Figure 6c. The tVOC concentration after the denuder is zero, indicative of the efficient removal of s/VOCs. Furthermore, SEM images of the released aerosol ($PM_{0.1–2.5}$) passed through the

thermal denuder (Figure 6d) show the nano-features and the characteristic large agglomerates and further confirm the absence of CNTs.

In addition. the ^{1}H-NMR spectra of aerosol samples with (route II) and without (route I) further process/treatment with the thermal denuder were obtained (Supporting Information, Figure S8). NMR spectroscopy provides detailed information for ultra-complex samples, as a whole, in a non-destructive and repeatable manner.[54] The mean of non-exchangeable organic hydrogen concentrations for the seven regions, OC concentration and molar H/C ratio are presented in Table 1. The total non-exchangeable organic hydrogen concentration were 223.8 μmol/m^3 and 86.4 μmol/m^3 of released aerosol in routes I and II, respectively, indicating a reduction of approximately 61.4%. In addition, quantitative differences were observed for the seven different types of organic hydrogen for the two routes of treatment (Supporting Information for more details). These changes clearly demonstrated the alteration of the chemical composition of released organic aerosol by the use of thermal denuder by removing compounds with amino, imino, unsaturated and aromatic-Hs as compared to those with strong aliphatic content.

Effect of thermal conditioner on the released aerosol—The further treatment of the released aerosol through the thermal conditioner (route III in Figure 1) also offers important information on the released aerosol properties. As presented above, the released aerosol from the TD of PU-CNT nanocomposite mostly consists of s/VOCs and other organic compounds. Therefore, this additional heat processing inside the thermal conditioner at a prolonged residence time (> 5 s) and high temperatures (800 °C) will facilitate the full combustion of the released aerosol. That would result in a complete TD of the released aerosol. By monitoring the particle number concentration at the exit of the thermal conditioner at both nano- and micron-sized regime (Figure 1, SMPS and APS), it was confirmed that the released aerosol from TD of PU-CNT at $T_{d,final}$ = 800 °C is fully combusted (data not shown).

Environmental impact and outlook

The main target of this study was to develop a versatile, integrated, exposure generation system for the standardized, controlled investigation of the TD of NEPs. The developed system consists of various modules that facilitate the controlled TD of NEPs in order to assess possible release of nanofillers and characterize the physicochemical morphological and toxicological properties of byproducts. The simplicity and versatility of INEXS platform allows its implementation by other laboratories (academic and industrial) worldwide and facilitate an inter-laboratory comparison of obtained results on TD of NEPs.

The INEXS does not aim to simulate an industrial incinerator, but to obtain a fundamental understanding on the thermal decomposition process of nano-enabled products and link important parameters to physicochemical, morphological and toxicological properties of byproducts. The suitability of the developed INEXS in life-cycle characterization studies was demonstrated here with a model NEP, *i.e.* polyurethane filled with carbon nanotubes (PU-CNT). There are no CNTs detected in the released aerosol at $T_{d,final}$ = 500 and 800 °C. In contrast, the residual ash at $T_{d,final}$ = 500 °C contains a large fraction, if not all, of the

initial CNTs that were present in the NEP. The residual ash after the thermal decomposition of the matrix at $T_{d,final}$ = 500 °C was a brittle material with CNT protrusions on its surface. Such a structure raises concerns for possible release in environmental media in the case of a landfill disposal, but one must also consider that commercial waste incineration employs temperatures above 800°C, for which we found no ash. The use of the thermal denuder confirmed the primary formation mechanism of the organic nanoparticles in the released aerosol and will enable in the future to assess potential toxicological implications derived from organic compounds. The additional heating step (thermal conditioner) which simulates commercial incinerator facilities further confirms the full combustion of the released carbonaceous aerosol. We employed one industry-relevant NEP in this study in order to provide proof-of-concept for the suitability of the developed methodology to study this important life-cycle scenario. A detailed investigation of thermal decomposition of thermoplastic materials will be reported in future manuscripts in order to assess how specific properties of NEPs and process conditions influence the potential nano-release and potential toxicological implications.

Future research is crucial in order to fully understand the TD of families of industry relevant NEPs and the potential release of nanofillers used in the synthesis of NEPs. More specifically, INEXS will be used to investigate the possible release of nanofillers from industry-relevant NEPs and assess the physicochemical and toxicological properties of the released byproducts. Assessing the potential toxicological effect from these byproducts will facilitate the development of a science-based regulatory framework for NEPs based on properties of realistic exposures rather than the properties of raw materials used in the NEP synthesis.

In particular, special emphasis should be given in studying industry-relevant NEPs with inorganic fillers (e.g. TiO_2, Fe_2O_3, Ag). In contrast to CNTs that fully decompose at moderate temperatures (below 800 °C) and O_2-rich conditions, inorganic materials will not fully decompose indicating that these NEPs will generate residual ash also at the higher temperatures. Furthermore, the fact that in this study there was no nanofiller (CNT) present in the released aerosol does not necessarily mean that this is the case for all NEPs in the market and for all nanofiller loading conditions and matrices used in the synthesis of NEPs. The specific effect of realistic mixed wastes and the total nanofiller concentration in the NEP on the released aerosol and residual ash characteristics needs to be further investigated to reach a conclusion on waste incineration. Different O_2/N_2 ratio in the inlet gas should also be employed in order to simulate the partial combustion conditions of incidental fires. It should be noted that if O_2-lean conditions (*i.e.* incomplete combustion) and/or NEPs with inorganic nanofillers (e.g. ceramics, metals) are decomposed, there should be detectable amount of residual ash at $T_{d,final}$ = 800 °C. It is also worth noting that in-vitro toxicological characterization studies performed with released size fractionated PM collected using the INEXS platform will be presented in future manuscripts for specific families of NEPs and thermal decomposition conditions. Particularly interesting scenario for investigation would be the fate transport of the residual ash in the environment following their placement in landfills after the NEP incineration. Finally, the obtained knowledge from such experiments will be exploited by industry in order to design safer NEPs with minimal adverse EHS

effects (e.g. safer coatings on nanofillers) towards a more responsible and sustainable nanotechnology.

Supplementary Material

Refer to Web version on PubMed Central for supplementary material.

Acknowledgments

We thank the FP7-MARINA consortium for kind provision of the PU materials. We kindly thank Dr. Martin Shafer (Univ. Wisconsin-Madison) for the EC/OC and ICP-MS measurements. This research was supported by NSF (grant nr. 1436450), NIH (grant nr. P30ES000002) and BASF AG. This work was performed in part at the Harvard Center for Nanoscale Systems (CNS), a member of the National Nanotechnology Infrastructure Network (NNIN), which is supported by the National Science Foundation under NSF award number ECS-0335765. Georgios A. Sotiriou gratefully acknowledges the Swiss National Science Foundation for the Advanced Researcher fellowship (grant nr. 145392).

ABBREVIATIONS

APS	aerodynamic particle sizer
CCI	compact cascade impactor
CNTs	carbon nanotubes
EC	elemental carbon
EHS	environmental health and safety
ENMs	engineered nanomaterials
HEPA	high-efficiency particulate air
ICP-MS	inductively coupled plasma mass spectrometry
LC	life-cycle
NEPs	nano-enabled products
OC	organic carbon
PM	particulate matter
PU	polyurethane
^{1}H-NMR	Proton nuclear magnetic resonance spectroscopy
SEM	scanning electron microscopy
SMPS	scanning mobility particle sizer
sVOCs	semi-volatile organic compounds
TD	thermal decomposition
TEM	transmission electron microscopy
tVOCs	total volatile organic compounds
VOCs	volatile organic compounds

References

1. Moniruzzaman M, Winey KI. Macromolecules. 2006; 39(16):5194–5205.
2. Roco, MC.; Mirkin, CA.; Hersam, MC. Nanotechnology Research Directions for Societal Needs in 2020. Springer; 2011.
3. Pyrgiotakis G, McDevitt J, Yamauchi T, Demokritou P. J Nanopart Res. 2012; 14(8):1027.
4. Kokonou M, Rebholz C, Giannakopoujos KP, Doumanidis CC. Microelectron Eng. 2008; 85(5–6): 1186–1188.
5. Bello D, Martin J, Santeufemio C, Sun Q, Lee Bunker K, Shafer M, Demokritou P. Nanotoxicology. 2012; 7(5):989–1003. [PubMed: 22551088]
6. Pirela SV, Pyrgiotakis G, Bello D, Thomas T, Castranova V, Demokritou P. Inhal Toxicol. 2014; 26(7):400–408. [PubMed: 24862974]
7. Pirela SV, Sotiriou GA, Bello D, Shafer M, Lee Bunker K, Castranova V, Thomas T, Demokritou P. Nanotoxicology. 2014 in press. 10.3109/17435390.2014.976602
8. Drakonakis VM, Velisaris CN, Seferis JC, Doumanidis CC, Wardle BL, Papanicolaou GC. Polym Compos. 2010; 31(11):1965–1976.
9. Pillai SK, Hadjiafxenti A, Doumanidis CC, Ando T, Rebholz C. Int J Appl Ceram Technol. 2012; 9(1):206–213.
10. Polychronopoulou K, Rebholz C, Baker MA, Theodorou L, Demas NG, Hinder SJ, Polycarpou AA, Doumanidis CC, Boebel K. Diam Relat Mat. 2008; 17(12):2054–2061.
11. Sotiriou GA, Diaz E, Long MS, Godleski J, Brain J, Pratsinis SE, Demokritou P. Nanotoxicology. 2012; 6(6):680–690. [PubMed: 21809902]
12. Nel A, Xia T, Madler L, Li N. Science. 2006; 311(5761):622–627. [PubMed: 16456071]
13. Demokritou P, Gass S, Pyrgiotakis G, Cohen JM, Goldsmith W, McKinney W, Frazer D, Ma J, Schwegler-Berry D, Brain J, Castranova V. Nanotoxicology. 2013; 7(8):1338–1350. [PubMed: 23061914]
14. Wiesner MR. Water Sci Technol. 2006; 53(3):45–51. [PubMed: 16605016]
15. Pratsinis A, Hervella P, Leroux JC, Pratsinis SE, Sotiriou GA. Small. 2013; 9(15):2576–2584. [PubMed: 23418027]
16. Konduru NV, Murdaugh KM, Sotiriou GA, Donaghey TC, Demokritou P, Brain JD, Molina RM. Part Fibre Toxicol. 2014; 11(1):44. [PubMed: 25183210]
17. Molina RM, Konduru NV, Jimenez RJ, Pyrgiotakis G, Demokritou P, Wohlleben W, Brain JD. Environ Sci: Nano. 2014 in press. 10.1039/C4EN00034J
18. Cohen JM, Derk R, Rojanasakul L, Godleski J, Kobzik L, Brain J, Demokritou P. Nanotoxicology. 2014; 8(S1):216–225. [PubMed: 24479615]
19. Landsiedel R, Ma-Hock L, Hofmann T, Wiemann M, Strauss V, Treumann S, Wohlleben W, Groters S, Wiench K, van Ravenzwaay B. Part Fibre Toxicol. 2014; 11(1):16. [PubMed: 24708749]
20. Hamilton RF Jr, Wu N, Porter D, Buford M, Wolfarth M, Holian A. Part Fibre Toxicol. 2009; 6(35)
21. Cohen JM, DeLoid G, Pyrgiotakis G, Demokritou P. Nanotoxicology. 2013; 7(4):417–431. [PubMed: 22393878]
22. Larsen ST, Roursgaard M, Jensen KA, Nielsen GD. Basic Clin Pharmacol Toxicol. 2010; 106(2): 114–117. [PubMed: 19874288]
23. Li JJ, Muralikrishnan S, Ng CT, Yung LYL, Bay BH. Exp Biol Med. 2010; 235(9):1025–1033.
24. Poland CA, Duffin R, Kinloch I, Maynard A, Wallace WAH, Seaton A, Stone V, Brown S, MacNee W, Donaldson K. Nat Nanotechnol. 2008; 3(7):423–428. [PubMed: 18654567]
25. Johnston HJ, Hutchison G, Christensen FM, Peters S, Hankin S, Stone V. Critical Rev Toxicol. 2010; 40(4):328–346. [PubMed: 20128631]
26. Nel AE, Maedler L, Velegol D, Xia T, Hoek EMV, Somasundaran P, Klaessig F, Castranova V, Thompson M. Nat Mater. 2009; 8(7):543–557. [PubMed: 19525947]

27. NNI. 2011 Environmental, Health, and Safety (EHS) Research Strategy. National Science and Technology Council Committee on Technology Subcommittee on Nanoscale Science, Engineering, and Technology; 2011.
28. A Research Strategy for Environmental, Health, and Safety Aspects of Engineered Nanomaterials. Committee to Develop a Research Strategy for Environmental, Health, and Safety Aspects of Engineered Nanomaterials; National Research Council; Washington, D.C: 2012.
29. Nowack B, David RM, Fissan H, Morris H, Shatkin JA, Stintz M, Zepp R, Brouwer D. Environ Int. 2013:591–11.
30. Bello D, Wardle BL, Yamamoto N, deVilloria RG, Garcia EJ, Hart AJ, Ahn K, Ellenbecker MJ, Hallock M. J Nanopart Res. 2009; 11(1):231–249.
31. Bello D, Wardle BL, Zhang J, Yamamoto N, Santeufemio C, Hallock M, Virji MA. Int J Occup Environ Health. 2010; 16(4):434–450. [PubMed: 21222387]
32. Goehler D, Stintz M, Hillemann L, Vorbau M. Ann Occup Hyg. 2010; 54(6):615–624. [PubMed: 20696941]
33. Koponen IK, Jensen KA, Schneider T. J Expo Sci Environ Epidemiol. 2011; 21(4):408–418. [PubMed: 20485339]
34. Kuhlbusch TAJ, Asbach C, Fissan H, Goehler D, Stintz M. Part Fibre Toxicol. 2011; 8(22)
35. Peters TM, Elzey S, Johnson R, Park H, Grassian VH, Maher T, O'Shaughnessy P. J Occup Environ Hyg. 2009; 6(2):73–81. [PubMed: 19034793]
36. Wohlleben W, Brill S, Meier MW, Mertler M, Cox G, Hirth S, von Vacano B, Strauss V, Treumann S, Wiench K, Ma-Hock L, Landsiedel R. Small. 2011; 7(16):2384–2395. [PubMed: 21671434]
37. Wohlleben W, Meier MW, Vogel S, Landsiedel R, Cox G, Hirth S, Tomovic Z. Nanoscale. 2013; 5(1):369–380. [PubMed: 23172121]
38. Bouillard J, R'Mili B, Moranviller D, Vignes A, Le Bihan O, Ustache A, Bomfim JS, Frejafon E, Fleury D. J Nanopart Res. 2013; 15(4):1–11.
39. Keller AA, McFerran S, Lazareva A, Suh S. J Nanopart Res. 2013; 15(6):1–17.
40. Keller AA, Lazareva A. Environ Sci Technol Lett. 2013; 1(1):65–70.
41. Walser T, Limbach LK, Brogioli R, Erismann E, Flamigni L, Hattendorf B, Juchli M, Krumeich F, Ludwig C, Prikopsky K, Rossier M, Saner D, Sigg A, Hellweg S, Guenther D, Stark WJ. Nat Nanotechnol. 2012; 7(8):520–524. [PubMed: 22609690]
42. Vejerano EP, Leon EC, Holder AL, Marr LC. Environ Sci: Nano. 2014; 1(2):133–143.
43. Gass S, Cohen JM, Pyrgiotakis G, Sotiriou GA, Pratsinis SE, Demokritou P. ACS Sustainable Chem Eng. 2013; 1(7):843–857. [PubMed: 23961338]
44. Sotiriou GA, Watson C, Murdaugh KM, Pyrgiotakis G, Elder A, Brain JD, Demokritou P. Environ Sci: Nano. 2014:1144–153.
45. Schneider J, Weimer S, Drewnick F, Borrmann S, Helas G, Gwaze P, Schmid O, Andreae MO, Kirchner U. Int J Mass Spectrom. 2006; 258(1–3):37–49.
46. Clarke, MJ.; Kadt, M.; Saphire, D.; Golden, SR. Burning garbage in the US: Practice vs state of the art. INFORM; New York, NY: 1991.
47. Demokritou P, Lee SJ, Ferguson ST, Koutrakis P. J Aerosol Sci. 2004; 35(3):281–299.
48. Khatri M, Bello D, Pal AK, Cohen JM, Woskie S, Gassert T, Lan J, Gu AZ, Demokritou P, Gaines P. Part Fibre Toxicol. 2013; 10(42)
49. Chang C, Demokritou P, Shafer M, Christiani D. Environ Sci-Process Impacts. 2013; 15(1):214–224. [PubMed: 24592438]
50. Woolley WD, Raftery MM. J Hazard Mater. 1976; 1(3):215–222.
51. Lehman JH, Terrones M, Mansfield E, Hurst KE, Meunier V. Carbon. 2011; 49(8):2581–2602.
52. Mansfield E, Kar A, Hooker S. Anal Bioanal Chem. 2010; 396(3):1071–1077. [PubMed: 20016881]
53. Matuszak ML, Frisch KC. J Polym Sci Pol Chem. 1973; 11(3):637–648.
54. Chalbot M-CG, Kavouras IG. Environ Poll. 2014:191232–249.

Nano impact statement

Nano-enabled products (NEPs) appear continuously in the market and it is therefore inevitable that a large fraction of those will reach their end-of-life by thermal decomposition. There are, however, important knowledge gaps regarding the outcomes from the thermal decomposition of NEPs, and more specifically regarding the potential nano-release and possible environmental health implications. In this manuscript, we present the development of a standardized, versatile, and reproducible methodology suitable for the systematic characterization of the physicochemical and toxicological properties of thermally-degraded industry-relevant NEPs. Such a methodology will facilitate detailed studies regarding the nano-emissions from the thermal decomposition of NEPs and will set the basis for regulators that aim to develop a science-based framework for NEPs based on properties of released byproducts rather than the properties of raw materials used in the NEP synthesis.

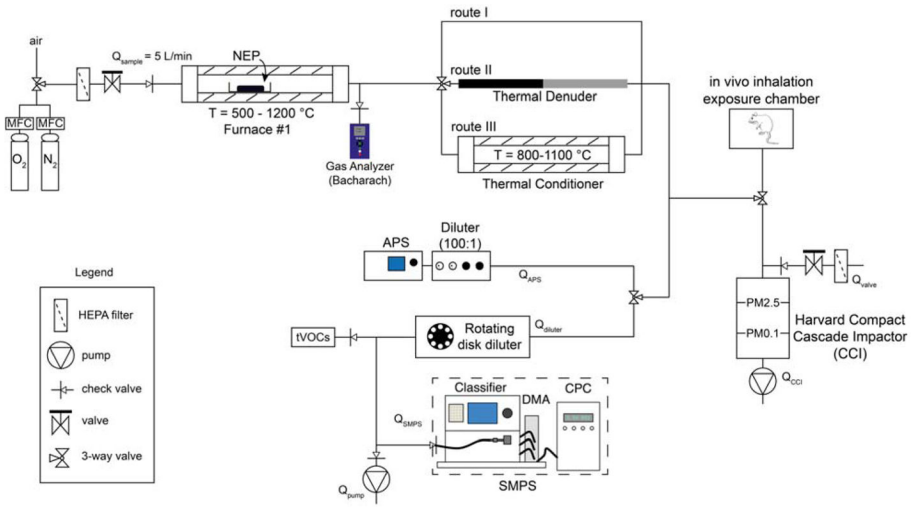

Figure 1.

The integrated exposure generation system (INEXS). The NEP is placed in a crucible in furnace #1, in which the temperature is finely controlled as well as its inlet gas composition (HEPA-filtered air or of controlled N_2/O_2 ratio). Upon the TD of the NEP, the released aerosol travels through three different routes (I–III) and *in situ* analyzed by a number of real-time instruments. Furthermore, the released aerosol can be collected and size-fractionated using the Harvard CCI. For future studies, the released aerosol can be directly guided in the *in vivo* inhalation chambers for toxicological analysis.

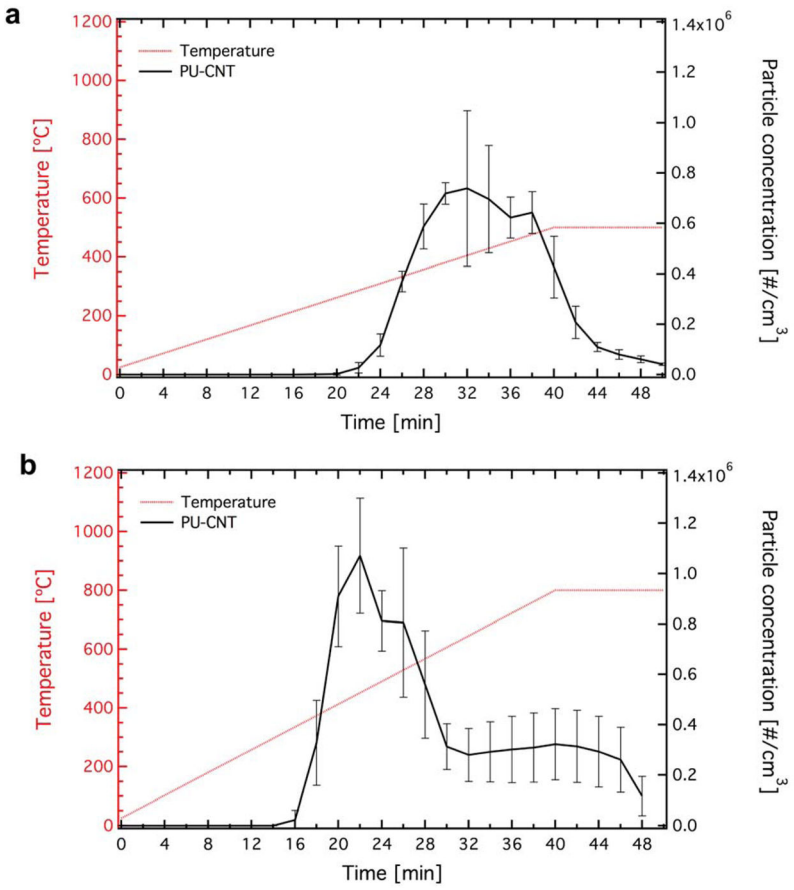

Figure 2.

The temperature evolution over time (red line, left axis) and the mobility particle concentration upon the TD of PU-CNT at $T_{d,final}$ = 500 (a) and 800 °C (b) after 100 times dilution.

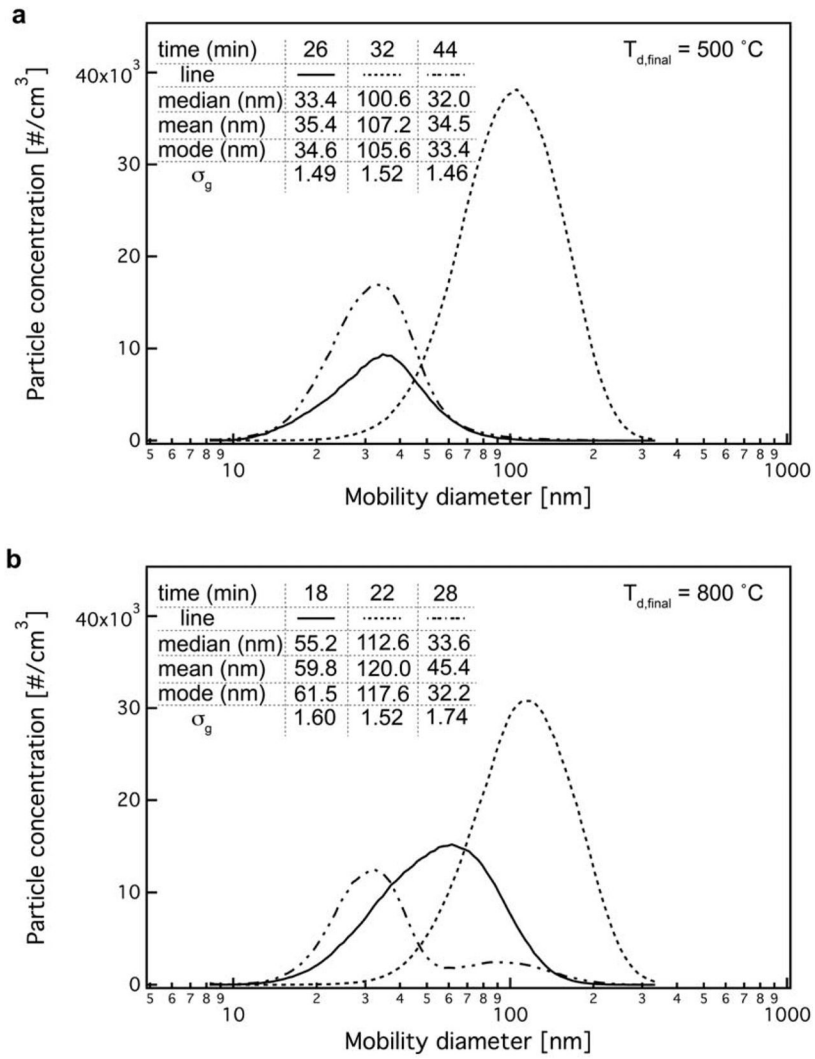

Figure 3.

The mobility particle size distributions of released aerosol upon the TD of PU-CNT at $T_{d,final}$ = 500 (a) and 800 °C (b) after 100 times dilution at three different time points, with their corresponding statistical analysis.

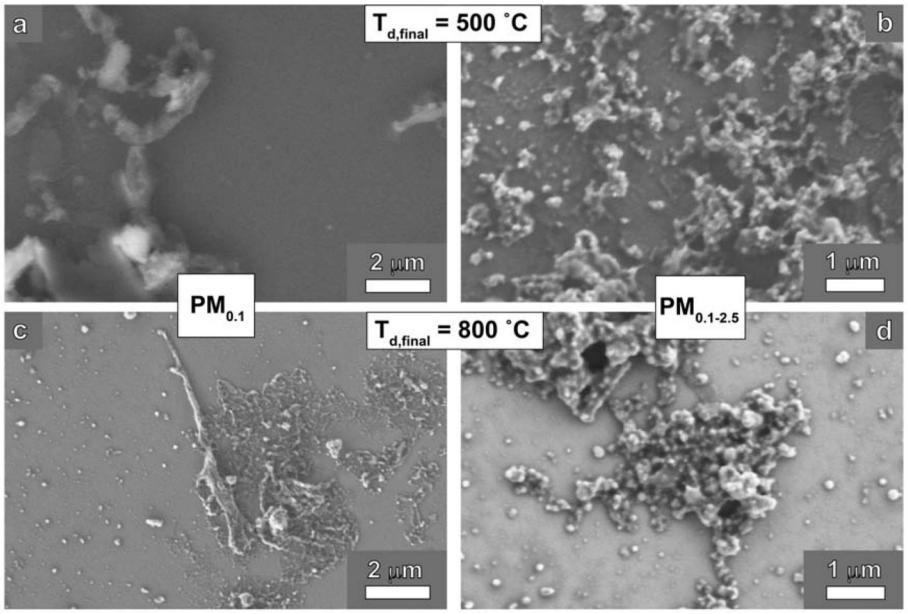

Figure 4.

SEM images of the released aerosol after extraction in EtOH of $PM_{0.1}$ (a,c) and $PM_{0.1–2.5}$ (b,d) for $T_{d,final}$ = 500 (a,b) and 800 °C (c,d).

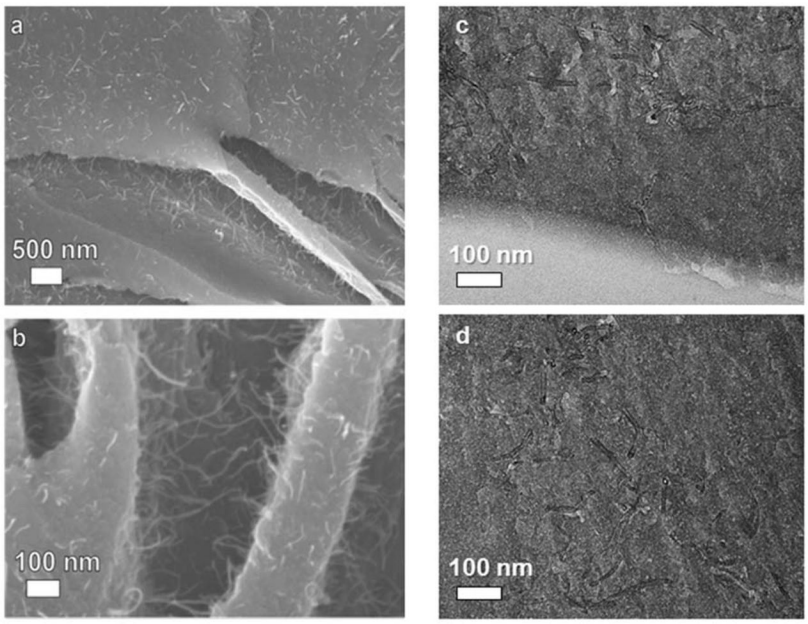

Figure 5.

Low (a) and high magnification (b) SEM images of residual ash after the TD of PU-CNT at $T_{d,final}$ = 500 °C, as well as top (c) and cross-sectional (d) TEM images revealing the homogeneous presence of CNTs.

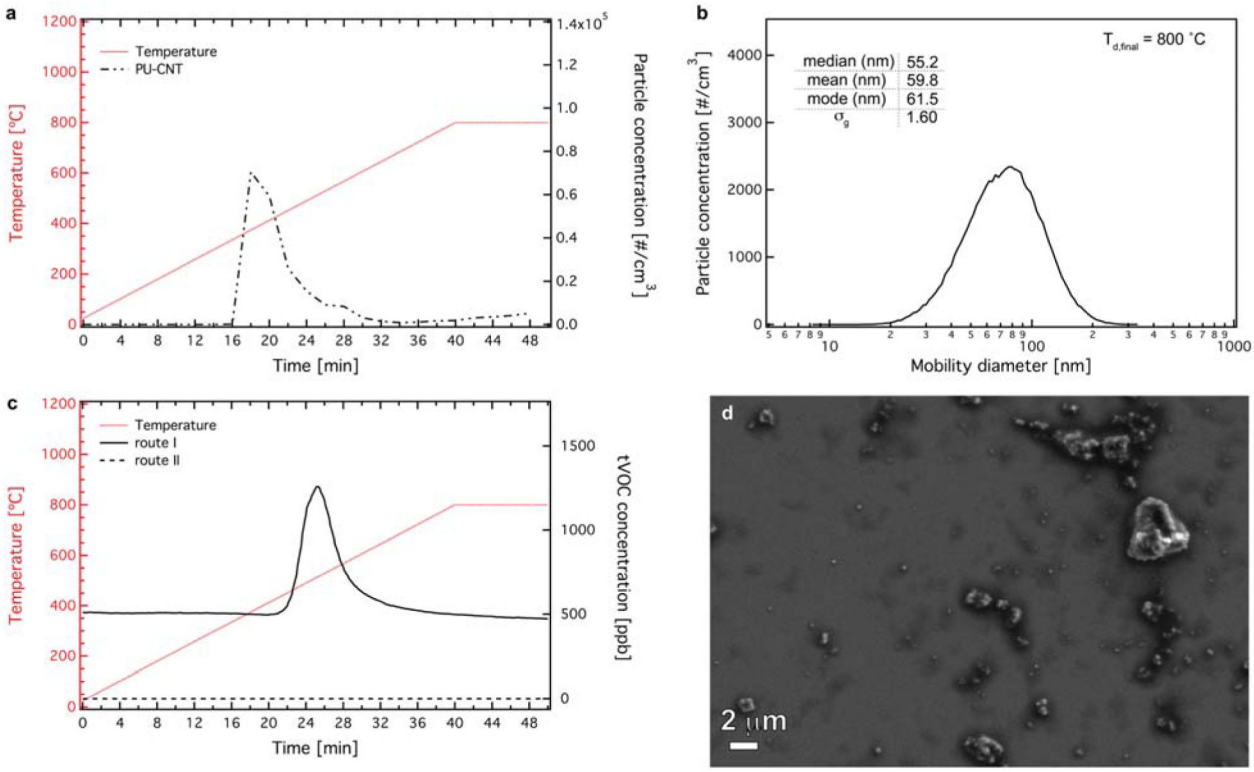

Figure 6.

The mobility particle concentration (a) and the size distribution (b) at the maximum concentration of the released aerosol upon the TD of PU-CNT at $T_{d,final}$ = 800 °C after 100 times dilution passing through the thermal denuder (route II in Figure 1). (c) The tVOC concentration of the released aerosol upon the TD of PU-CNT at $T_{d,final}$ = 800 °C after 100 times dilution from route I (solid line, before the denuder) and route II (broken line, after denuder). (d) A SEM image of the extracted $PM_{0.1–2.5}$ released aerosol from route II at $T_{d,final}$ = 800 °C.

Table 1

Total non-exchangeable organic hydrogen content of released aerosol extracted from samples collected during the TD of PU-CNT at at $T_{d,final}$ = 800 °C from routes I (without the thermal denuder) and II (with the thermal denuder).

	Route I	**Route II**
Total H content (μmol/m^3)	223.8	84.4
*% (R-**H**)* (0.5–1.8 ppm)	42.7	62.7
*% (=C-C-**H**) (1.8–3.1 ppm)*	26.1	17.5
*% (O-C-**H** and O-**H**) (3.5–4.6 ppm)*	7.7	5.4
*% (H-C=C-**H**) (4.6–6.5 ppm)*	7.1	3.0
*% (Ar-**H**) (6.5–8.5 ppm)*	13.7	9.6
*% (**H**-C=N) (8.5–10.9 ppm)*	2.5	1.8
*% (COO**H** and Ar-O**H**) (10.9–12.4 ppm)*	0.3	0.1
WSOC (μmol/m^3)	96.7	36.3
H/C molar ratio	2.31	2.38